

TRAJECTORY DESIGN FOR A SOLAR POLAR OBSERVING CONSTELLATION

Thomas R. Smith^{*}, Natasha Bosanac[†], Thomas E. Berger[‡], Nicole Duncan[§], and Gordon Wu[¶]

Space-based observatories are an invaluable resource for forecasting geomagnetic storms caused by solar activity. Currently, most space weather satellites obtain measurements of the Sun's magnetic field along the Sun-Earth line and in the ecliptic plane. To obtain complete and regular polar coverage of the Sun's magnetic field, the University of Colorado Boulder's Space Weather Technology, Research, and Education Center (SWx TREC) and Ball Aerospace are currently developing a mission concept labeled the Solar Polar Observing Constellation (SPOC). This concept comprises two spacecraft in low-eccentricity and high-inclination heliocentric orbits at less than 1 astronomical unit (AU) from the Sun. The focus of this paper is the design of a trajectory for the SPOC concept that satisfies a variety of hardware and mission constraints to improve solar magnetic field models and wind forecasts via polar viewpoints of the Sun.

INTRODUCTION

Space weather satellites are essential in developing accurate solar magnetic field models and solar wind forecasts to provide advance warnings of geomagnetic storms. Measurements of the solar magnetic field are the primary inputs to forecasts of the solar wind and, thus, the arrival times of coronal mass ejections (CMEs). Space-based magnetogram and doppler velocity measurements of the Sun's magnetic field are valuable in developing these models and forecasts. Currently, most space weather satellites obtain measurements along the Sun-Earth line and within the ecliptic plane, e.g., Solar and Heliospheric Observatory (SOHO) and Solar Dynamics Observatory (SDO).^{1,2} However, these satellites only obtain measurements of the Earth-facing side of the Sun at a given instant in time and cannot directly observe the polar regions of the Sun where the majority of high-speed solar wind streams originate.³ Continuous space weather monitoring and long-term helioseismic observations need to be conducted in a stable low-eccentricity and high-inclination heliocentric orbit to achieve long time-average studies (weeks-to-months) of the polar convection zone. Therefore, observations of the Sun from additional vantage points, particularly with better measurements of the solar poles, are necessary to obtain continuous, complete, and accurate measurements of the Sun's magnetic field to improve solar wind forecasts and provide advance geomagnetic storm warnings.³⁻⁵

^{*}Graduate Research Assistant, Colorado Center for Astrodynamics Research, Smead Department of Aerospace Engineering Sciences, University of Colorado Boulder, Boulder, CO 80309.

[†]Assistant Professor, Colorado Center for Astrodynamics Research, Smead Department of Aerospace Engineering Sciences, University of Colorado Boulder, 431 UCB, Boulder, CO 80309.

[‡]Director, Space Weather Technology, Research, and Education Center, College of Engineering and Applied Science, University of Colorado Boulder, Boulder, CO 80309.

[§]Advanced Systems Manager for Heliophysics, Ball Aerospace & Technologies Corporation, Boulder, CO 80301.

[¶]Principal Spacecraft Engineer, Ball Aerospace & Technologies Corporation, Boulder, CO 80301.

The need for more complete observations of the Sun from outside the ecliptic plane has motivated the development of a variety of mission concepts. One key to these mission concepts is the design of trajectories that can achieve a high inclination with respect to the ecliptic within both a reasonable time frame and the spacecraft hardware constraints. Potential options for achieving a high-inclination heliocentric orbit with respect to the ecliptic plane include, but are not limited to, orbit inclination cranking, a Jupiter gravity assist (JGA), and gravity assist sequences involving Earth and Venus. For instance, the Solar Polar Imager (SPI), Solar Polar Diamond Explorer (SPDEX), and POLAR Investigation of the Sun (POLARIS) concepts all leverage a solar sail and orbit inclination cranking to achieve a low-eccentricity and high-inclination heliocentric orbit for either one or multiple spacecraft.⁶⁻⁸ The European Space Agency's Solar Orbiter mission plans to study the Sun at high latitudes using a series of Earth and Venus flybys.⁹ The Telemachus and Solar Polar Explorer (SOLPEX) concepts, however, use a JGA to provide the heliocentric inclination change needed to obtain a polar perspective of the Sun.^{10,11} In addition, the University of Colorado Boulder's Space Weather Technology, Research, and Education Center (SWx TREC) and Ball Aerospace are currently developing a mission concept, the Solar Polar Observing Constellation (SPOC), that utilizes a JGA in the trajectory design. The goal of the mission is to place a constellation of spacecraft in low-eccentricity and nearly polar heliocentric orbits within the radius of Earth's orbit. A polar heliocentric orbit offers the required coverage of the Sun's polar regions while the constellation ensures regular measurements of both the poles and viewpoints that are off the Sun-Earth line. The SPOC mission concept is designed to make long-term helioseismic and magnetic field measurements of the polar regions of the Sun, enabling both continuous long-term discovery science and operational space weather monitoring in the same mission.³

Drawing inspiration from the Ulysses and Dawn missions, the SPOC mission concept leverages a JGA to insert a spacecraft into a nearly polar heliocentric orbit. The Ulysses spacecraft provides some initial precedent in pursuit of a high-inclination orbit with respect to the ecliptic: the spacecraft achieved a highly eccentric, high-inclination heliocentric orbit using a JGA.¹² The Ulysses mission demonstrated an efficient ballistic method for achieving a large inclination with respect to the Sun. However, the final orbit of the Ulysses spacecraft was highly eccentric with a periapsis radius of approximately 1.4 astronomical units (AU) and an apoapsis radius of approximately 5.4 AU. The SPOC mission concept requires a low-eccentricity heliocentric orbit within the radius of Earth's orbit to ensure regular polar passes. Unlike Ulysses, the SPOC spacecraft would require significant propulsive maneuvers to reduce the size of the heliocentric orbit after the JGA. Rather than using chemical propulsion, solar electric propulsion (SEP) reduces the propellant mass required to achieve this significant change in the orbit; the Dawn mission demonstrated the value of this approach.¹³ Together, the trajectories leveraged by the Ulysses and Dawn missions provide historical foundation for developing a viable trajectory solution for the SPOC mission concept.

Achieving a low-eccentricity and nearly polar heliocentric orbit within the radius of Earth's orbit requires a trajectory design approach that incorporates constraints based on mission objectives, secondary science goals, launch conditions, and spacecraft hardware. For the SPOC mission concept, a constellation of two spacecraft is assumed for the initial design. The selected itinerary supports secondary science during the Jupiter flyby and several polar passes before each spacecraft reaches its operational orbit. The SPOC mission itinerary for the trajectory design of a single spacecraft is separated into two phases: Launch-to-JGA and JGA-to-Operational-Orbit. Selecting a trajectory in the Launch-to-JGA phase utilizes Lambert's problem to evaluate the design space of natural Earth to Jupiter transfers that lead to a large change in heliocentric inclination. The analysis of the design

space during this phase specifically focuses on ballistic transfers from Earth to Jupiter to eliminate the need for any large maneuvers before the JGA. In addition, the initial launch date is assumed to be in 2025, although future launch opportunities are available due to the synodic period of Earth and Jupiter. Then, to achieve the low-eccentricity operational orbit the spacecraft is equipped with three 25-cm Xenon Ion Propulsion System (XIPS-25) thrusters developed by L3 Communications to execute propulsive maneuvers after the JGA.¹⁴ In this paper, a multiple shooting corrections scheme is used to recover a continuous trajectory with a low-complexity thrust profile to achieve the final desired operational orbit. After developing a viable trajectory for a single spacecraft, phasing strategies are presented to achieve a configuration for two spacecraft to enable regular measurements of the Sun's magnetic field from new polar vantage points.

MISSION OVERVIEW

Trajectory Design Requirements

The primary objective of the SPOC mission concept is to obtain regular and complete measurements of the polar regions of the Sun's magnetic field. To achieve this objective, an operational constellation of spacecraft is placed in low-eccentricity and nearly polar heliocentric orbits within the radius of Earth's orbit using a JGA and long duration maneuvers via a SEP system. Each spacecraft in the constellation has a suite of onboard instruments including: a solar magnetograph, a solar coronagraph, and in-situ plasma and interplanetary magnetic field instruments.³ The trajectory design requirements established by SWx TREC and Ball Aerospace are derived directly from the primary objective of the mission as well as the technical specifications of these instruments. The final operational orbit of each spacecraft is required to have a semi-major axis less than 1 AU, an eccentricity less than or equal to 0.05, and a maximum solar latitude greater than 75°. To define a constellation for the purposes of the initial mission concept design, a minimum of two spacecraft are required to be phased in true anomaly by approximately 180° in operational orbits satisfying these requirements. A constellation of at least two spacecraft is required for operational redundancy and to obtain simultaneous measurements of both the north and south pole of the Sun. In addition, an interplanetary launch in 2025 from Cape Canaveral on a Falcon Heavy is assumed and a flight time of less than 8 years from launch to initial operations for each spacecraft is desired. Due to the synodic period of Earth and Jupiter, additional launch opportunities are available approximately every 400 days. Together, these requirements and considerations, current as of August 2019, are the main design drivers used in this paper to develop a viable trajectory solution for the SPOC concept.

Spacecraft Model

Trajectory design for the SPOC mission concept is dependent on the spacecraft hardware parameters, such as the total mass of a single spacecraft and SEP system configuration. The spacecraft design is being conducted by Ball Aerospace and a summary of relevant design drivers is outlined in Table 1. The SEP system is comprised of three XIPS-25 thrusters and the estimated throughput of each thruster is 134 kg when operated at full power.¹⁴ When the thrusters are activated simultaneously, the SEP system is capable of producing a total maximum thrust of 495 mN with an I_{sp} equal to 3550 seconds given a maximum thruster power of 12.8 kW. The current baseline dry mass for each spacecraft is 620 kg with an assumed maximum available propellant mass of 280 kg, resulting in an initial wet mass of 900 kg for each spacecraft. These configuration parameters sufficiently define the spacecraft model for use in a preliminary trajectory design process.

Table 1. Baseline SPOC Spacecraft Model

Parameter	Value
Dry Mass (kg)	620
Maximum Propellant Mass (kg)	280
Maximum Thrust (mN)	495
I_{sp} (s)	3550
Maximum Thruster Power (kW)	12.8

DYNAMICAL MODELS

The baseline itinerary for a single spacecraft in the SPOC mission concept consists of an Earth departure, an interplanetary cruise, a JGA, and, finally, long duration maneuvers to reach the final operational orbit around the Sun. This itinerary is described by two fundamental phases: Launch-to-JGA and JGA-to-Operational-Orbit. The initial design for the Launch-to-JGA phase is developed using a classical two-body model while design for the JGA-to-Operational-Orbit phase is developed using a SEP-enabled two-body model where the SEP system is only activated during the propulsive maneuvers. Using a patched conic approach that leverages the SEP system and the two-body problem offers a simplified, yet representative approximation of the dynamical environments throughout the mission and enables the construction of an initial guess. To increase the fidelity of the trajectory design analysis, the initial guess for a trajectory is transitioned into a SEP-enabled point mass ephemeris model including the gravitational influence of the Sun, Earth, Mars, Jupiter, and Saturn. Recovering a viable trajectory in a higher fidelity model is vital for demonstrating operational feasibility in the multi-body gravitational environment of the solar system.

SEP Model

A model describing a SEP system is necessary to incorporate its effect on the dynamics of a spacecraft. The thrust and mass flow rate produced by a SEP system depends on the amount of available power for the thrusters, which is a function of the distance of the spacecraft from the Sun.¹⁵ The maximum thruster power listed in Table 1 for a single SPOC spacecraft is assumed to be available when $r_{Sun,sc} \leq 1$ AU, where $r_{Sun,sc}$ is the distance between the Sun and the spacecraft. However, when the distance between the Sun and the spacecraft is greater than 1 AU the available thruster power, P_{Avail} , is defined as:

$$P_{Avail} = \frac{P_{Max}}{r_{Sun,sc}^2} \quad (1)$$

where P_{Max} is the maximum thruster power of the SEP system. The thruster efficiency, η , is computed as:

$$\eta = \frac{T_{Max} I_{sp} g_0}{2P_{Max}} \quad (2)$$

where T_{Max} is the maximum thrust produced by the SEP system, I_{sp} is the constant specific impulse of the SEP system, and g_0 is the gravitational acceleration on the surface of the Earth ($9.81 \frac{m}{s^2}$). Therefore, η is approximately equal to 0.6734 for the SEP system used in the SPOC mission

concept. The thrust, T , produced by the SEP system at any distance from the Sun is subsequently defined as:

$$T = \frac{2\eta P_{Avail}}{I_{sp}g_0} \quad (3)$$

and varies as the spacecraft is located at distances beyond 1 AU, when the available power is below the maximum value. Finally, the mass flow rate produced by the SEP system is defined as:

$$\dot{m} = \frac{-2\eta P_{Avail}}{(I_{sp}g_0)^2} \quad (4)$$

Since the mass flow rate varies according to the power available, the mass of the spacecraft, m , must be introduced as an additional state variable for the spacecraft in a SEP-enabled dynamical model. This parameterization of the SEP system offers an initial approximation of the thrust and mass flow rate of the thrusters for preliminary trajectory design. Of course, the complexity of this model should be increased as more information about the propulsion system is made publicly available.

SEP-Enabled Two-Body Model

A SEP-enabled two-body model is used to approximate the motion of a spacecraft with a SEP system operating primarily under the gravitational influence of the Sun.¹⁶ The Sun is modeled as a constant point mass while the spacecraft is assumed to possess a negligible mass relative to the Sun. Therefore, the spacecraft does not impact the motion of the Sun. The dimensional state vector for the spacecraft relative to the Sun in an inertial frame is written as $\vec{q} = [X, Y, Z, \dot{X}, \dot{Y}, \dot{Z}]$. The relative equations of motion for a spacecraft equipped with a SEP system are then written as:

$$\begin{aligned} \ddot{X} &= \frac{-\mu}{r_{Sun,sc}^3} X + \frac{T}{m} u_X \\ \ddot{Y} &= \frac{-\mu}{r_{Sun,sc}^3} Y + \frac{T}{m} u_Y \\ \ddot{Z} &= \frac{-\mu}{r_{Sun,sc}^3} Z + \frac{T}{m} u_Z \\ \dot{m} &= \frac{-2\eta P_{Avail}}{(I_{sp}g_0)^2} \end{aligned} \quad (5)$$

where μ is the standard gravitational parameter for the Sun-spacecraft two-body problem and $\hat{u} = [u_X, u_Y, u_Z]$ is the unit thrust vector of the spacecraft in the inertial frame. The thrust vector is initially defined in a velocity-normal-conormal (VNC) coordinate frame relative to the Sun to provide intuitive thrust directions.^{17,18} However, the thrust vector must be converted from the VNC frame to the Sun-centered inertial coordinate frame for use in the equations of motion as defined in Eq. 5. This SEP-enabled two-body model serves as the foundation for developing the initial trajectory design for the SPOC concept.

SEP-Enabled Point Mass Ephemeris Model

A SEP-enabled point mass ephemeris model is used in a higher fidelity representation of the motion of a spacecraft equipped with a SEP system and operating under the gravitational influence

of multiple attracting bodies.^{17,18} Similar to the SEP-enabled two-body model, each attracting body is approximated as a constant point mass, the spacecraft is assumed to have negligible mass relative to each of the bodies, and the motion of each body is defined relative to the same central body, i.e. the Sun. In an inertial frame, $\hat{X}\hat{Y}\hat{Z}$, the state of body j with respect to body i is written as $\vec{q}_{i,j} = [X_{i,j}, Y_{i,j}, Z_{i,j}, \dot{X}_{i,j}, \dot{Y}_{i,j}, \dot{Z}_{i,j}]$ for $i, j = \text{Sun, sc, etc.}$ Then, the dimensional state of the spacecraft relative to the Sun in an inertial frame is written as $\vec{q}_{Sun,sc} = \vec{q}_{sc} - \vec{q}_{Sun} = [X, Y, Z, \dot{X}, \dot{Y}, \dot{Z}]$. The resulting relative equations of motion for the spacecraft are written as:

$$\begin{aligned}
\ddot{X} &= \frac{-\mu}{r_{Sun,sc}^3} X + \sum_{j=3}^n \mu_j \left(\frac{X_{sc,j}}{r_{sc,j}^3} - \frac{X_{Sun,j}}{r_{Sun,j}^3} \right) + \frac{T}{m} u_X \\
\ddot{Y} &= \frac{-\mu}{r_{Sun,sc}^3} Y + \sum_{j=3}^n \mu_j \left(\frac{Y_{sc,j}}{r_{sc,j}^3} - \frac{Y_{Sun,j}}{r_{Sun,j}^3} \right) + \frac{T}{m} u_Y \\
\ddot{Z} &= \frac{-\mu}{r_{Sun,sc}^3} Z + \sum_{j=3}^n \mu_j \left(\frac{Z_{sc,j}}{r_{sc,j}^3} - \frac{Z_{Sun,j}}{r_{Sun,j}^3} \right) + \frac{T}{m} u_Z \\
\dot{m} &= \frac{-2\eta P_{Avail}}{(I_{sp}g_0)^2}
\end{aligned} \tag{6}$$

where n is the total number of bodies in the system (including the spacecraft), μ_j is the standard gravitational parameter of body j , $r_{i,j}$ is the distance between body i and body j , and $\hat{u} = [u_X, u_Y, u_Z]$ is the unit thrust vector of the spacecraft in the inertial frame. Consistent with the SEP-enabled two-body model, the unit thrust vector is converted from an intuitive description in the VNC frame to the Sun-centered inertial frame to produce \hat{u} . Additionally, the values of j in Eq. 6 range from 3 to n where each value of j corresponds to an attracting body included in the model (excluding the Sun and the spacecraft). For the SPOC mission concept design, $n = 6$ because the following additional attracting bodies are included in the model: Earth ($j = 3$), Mars ($j = 4$), Jupiter ($j = 5$), and Saturn ($j = 6$). Within this model, NASA's SPICE Toolkit is used to obtain the ephemerides of each planetary body.¹⁹ Transitioning a trajectory solution from a SEP-enabled two-body model to a SEP-enabled point mass ephemeris model is necessary to demonstrate the feasibility of the trajectory in a higher fidelity environment.

DESIGN APPROACH: LAUNCH TO JUPITER GRAVITY ASSIST

Interplanetary Transfer

The first phase of the SPOC mission itinerary is the Launch-to-JGA phase, capturing the path of the spacecraft including launch from the Earth, coasting towards Jupiter, and performing a natural flyby of Jupiter to change its heliocentric inclination with respect to the ecliptic plane. Assuming a launch year of 2025, direct natural transfers from Earth to Jupiter are evaluated by solving Lambert's problem for a range of Earth departure dates and a range of Jupiter arrival dates.¹⁷ The ephemerides of each planet for each pair of departure and arrival dates are obtained from NASA's SPICE Toolkit.¹⁹ The launch C_3 from Earth (red contours), the arrival v_∞ at Jupiter (blue contours), and the time of flight for each Earth to Jupiter transfer (black contours) is depicted in the porkchop plot in Figure 1 where the horizontal axis is the range of Earth departure dates and the vertical axis is the range of Jupiter arrival dates. Note that the characteristics of the computed transfers repeat approximately every 400 days, which is approximately the synodic period of Earth and Jupiter.

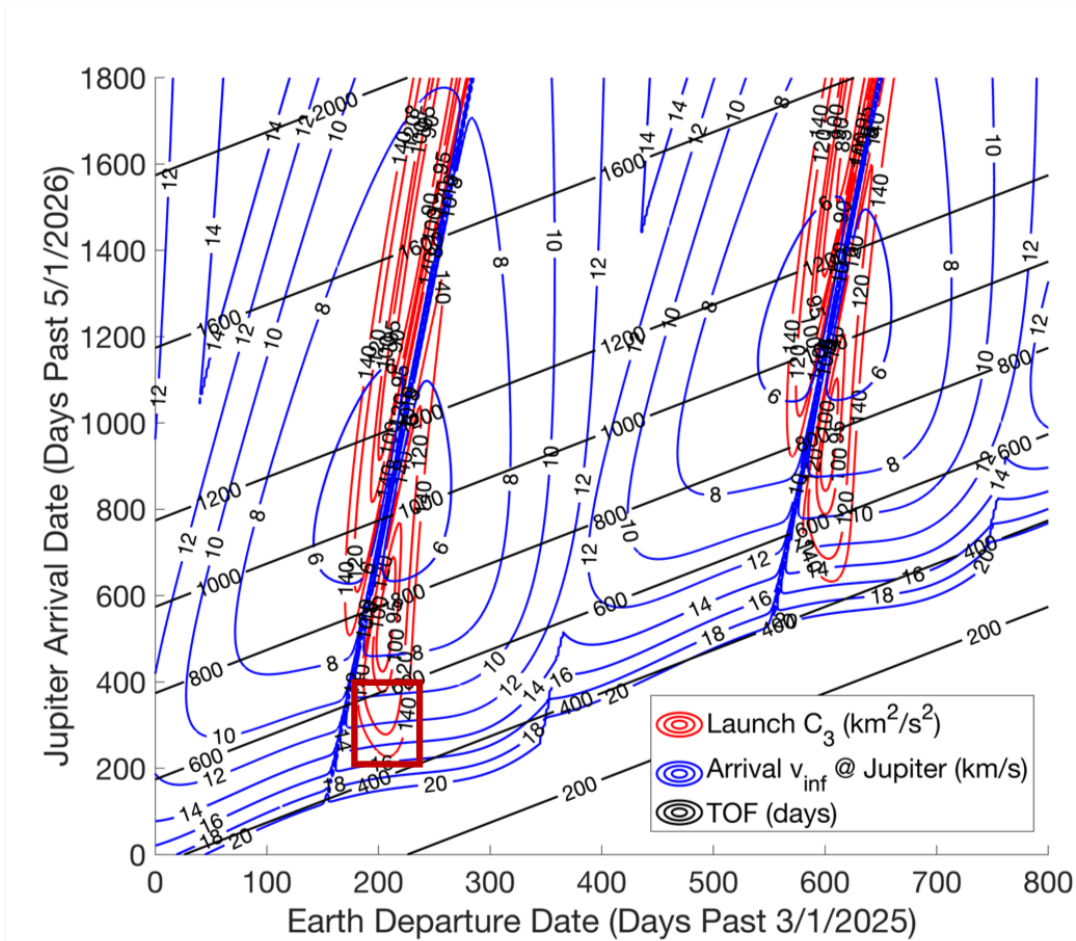


Figure 1. Porkchop plot capturing natural Earth to Jupiter transfers for departure dates beginning on 3/1/2025 and arrival dates beginning on 5/1/2026. A region of transfers for further analysis is highlighted in red.

Therefore, similar direct transfer opportunities from Earth to Jupiter are available nearly every year, offering flexibility in the SPOC mission architecture and enabling rapid design of similar transfers during subsequent launch opportunities after 2025. The Earth to Jupiter transfer must be designed to limit the time of flight and the launch C_3 while producing a JGA that achieves a large change in heliocentric inclination and a heliocentric periapsis radius of less than 1 AU. A large arrival v_∞ at Jupiter is used to achieve a large heliocentric inclination with respect to the ecliptic after the JGA. The natural transfers within the red highlighted region of the porkchop plot in Figure 1 are evaluated in a more detailed analysis because each solution has a desirable time of flight, a reasonable launch C_3 , and a large arrival v_∞ at Jupiter. Traditionally, the C_3 values in this region ($100\text{-}160 \frac{km^2}{s^2}$) would be considered large. However, in this analysis these C_3 values are considered feasible for a single SPOC spacecraft when launched on a Falcon Heavy based on predicted capabilities.

Jupiter Gravity Assist

The heliocentric inclination change achieved via a JGA depends on the geometry of the gravity assist as well as the properties of the direct interplanetary transfer from Earth to Jupiter. The

solutions to Lambert’s problem enable an initial identification of a region of candidate transfers from the Earth to Jupiter. However, a more detailed analysis is required to evaluate the achievable heliocentric inclinations post-JGA for each of the candidate transfers; GMAT is used to target solutions with the desired properties and to evaluate this design space.¹⁵ An Earth departure altitude equal to 300 km and an inclination equal to 28.5° relative to the Earth’s equator is assumed for each transfer based on launching from Cape Canaveral.²⁰ For each transfer, the initial state components of the outgoing hyperbolic trajectory from Earth are defined in GMAT in an Earth-centered J2000 Equatorial reference frame as:

$$\begin{aligned}
R_p &= 6678.1363 \text{ km} \\
C_3 &= \|\vec{v}_{\infty,Earth}\|^2 \\
RHA &= \tan^{-1} \left(\frac{v_{\infty,Earth_Y}}{v_{\infty,Earth_X}} \right) \\
DHA &= \tan^{-1} \left(\frac{v_{\infty,Earth_Z}}{\sqrt{v_{\infty,Earth_X}^2 + v_{\infty,Earth_Y}^2}} \right) \\
BVAZI &= \sin^{-1} \left(\frac{\cos(i)}{DHA} \right) \\
TA &= 0^\circ
\end{aligned} \tag{7}$$

where R_p is the radius of periapsis, $\vec{v}_{\infty,Earth} = [v_{\infty,Earth_X}, v_{\infty,Earth_Y}, v_{\infty,Earth_Z}]$ is the v_{∞} vector relative to Earth, RHA is the right ascension, DHA is the declination, $BVAZI$ is the B-vector azimuth at infinity, i is the inclination, and TA is the true anomaly of the trajectory relative to Earth.^{15,17,21} Note that if $BVAZI$ is a complex number, the transfer is not achievable from the assumed Earth departure inclination. Using these definitions, GMAT is leveraged to target B-plane parameters of the Jupiter gravity assist in a Jupiter-centered J2000 Ecliptic reference frame. A point mass ephemeris model including the Sun, Earth, Mars, Jupiter, and Saturn is used to integrate the path of the spacecraft from Earth departure to perijove. A small correction maneuver applied to the spacecraft at the initial Earth departure state is iteratively updated to target a specific set of Jupiter B-plane parameters. Trajectory correction maneuvers (TCMs) are not included during the interplanetary cruise from Earth to Jupiter at this stage of the trajectory design but would certainly be necessary post-launch to achieve a specific B-plane target at Jupiter.

Heliocentric orbit changes due to a planetary gravity assist are sensitive to the B-plane target of the gravity assist. To reduce the complexity of the design space for the JGA leveraged in the SPOC mission concept, a perijove equal to 450400 km (approximately 6.3 Jupiter radii) is assumed for all transfers and derived from the Jupiter flyby conditions along the Ulysses trajectory.²² A set of transfers departing the Earth between 9/8/2025 and 10/13/2025 and arriving at Jupiter between 12/10/2026 and 5/27/2027 are each computed in GMAT for a range of B-vector target angles from 90° to 175°. This analysis produced 2646 total transfers as depicted in Figure 2a) where the Earth departure date of each trajectory is plotted as a function of time of flight on the vertical axis and departure C_3 in color. The results of this evaluation are filtered based on post-JGA heliocentric inclination with respect to the ecliptic plane (85°-95°), post-JGA radius of periapsis relative to the Sun (0.5-1.0 AU), and departure C_3 ($< 135 \frac{km^2}{s^2}$). These filter ranges are selected based on the mission’s operational orbit requirements and current launch vehicle capabilities. After filtering the solution set, the remaining 29 candidate trajectories are plotted in Figure 2b). The post-JGA radius

of periapsis relative to the Sun and heliocentric inclination relative to the ecliptic plane for these filtered candidate trajectories are displayed in Figure 3a). Additionally, the post-JGA radius of periapsis relative to the Sun and the eccentricity for these solutions are plotted in Figure 3b). The two groups of data in these figures correspond to two different B-vector target angles for the JGA. The group with the smaller post-JGA heliocentric periapsis range have a B-vector target angle equal to 155° while the group with the larger periapsis range have a B-vector target angle equal to 150° . Following analysis of Figure 3b), a larger post-JGA heliocentric periapsis radius is desired because this grouping of trajectories has a lower eccentricity. Therefore, fewer propulsive adjustments are required to achieve a nearly circular heliocentric orbit via the SEP system.

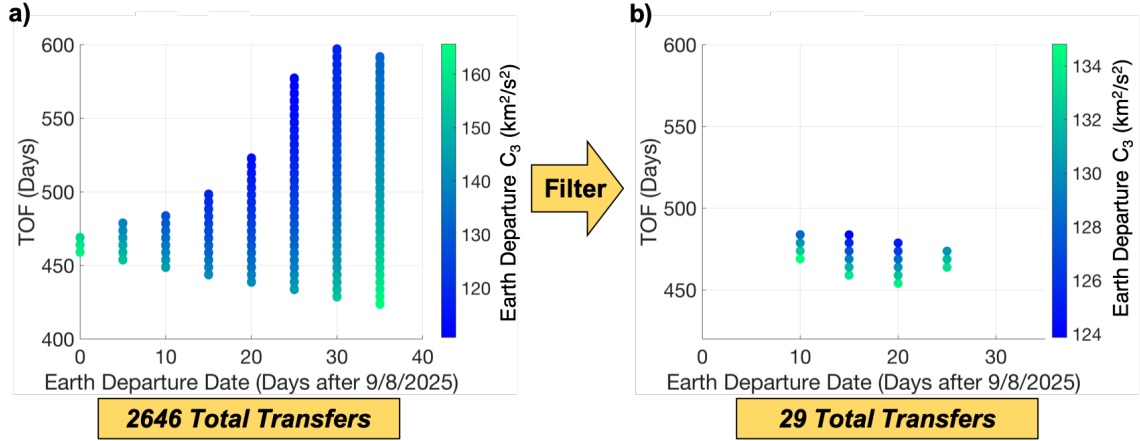


Figure 2. Candidate transfer trajectories from Earth to Jupiter computed in GMAT each for a range of B-vector target angles from 90° to 175° . The initial set of candidates a) are filtered based on post-JGA heliocentric inclination with respect to the ecliptic plane (85° - 95°), post-JGA radius of periapsis relative to the Sun (0.5-1.0 AU), and departure C_3 ($< 135 \frac{km^2}{s^2}$).

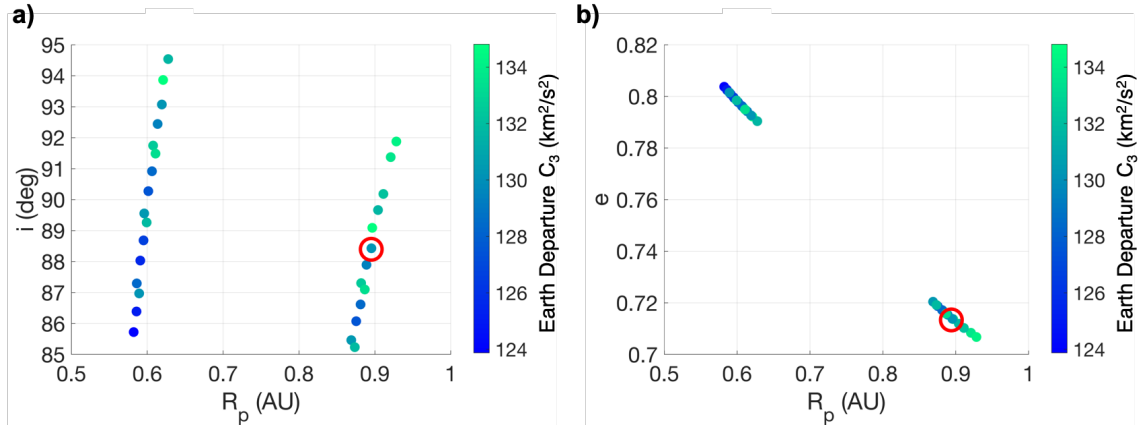


Figure 3. Post-JGA heliocentric orbit characteristics of the filtered candidate transfer trajectories displayed in Figure 2b). The radius of periapsis, R_p , and eccentricity, e , values are defined with respect to the Sun and the inclination, i , values are defined with respect to the ecliptic plane.

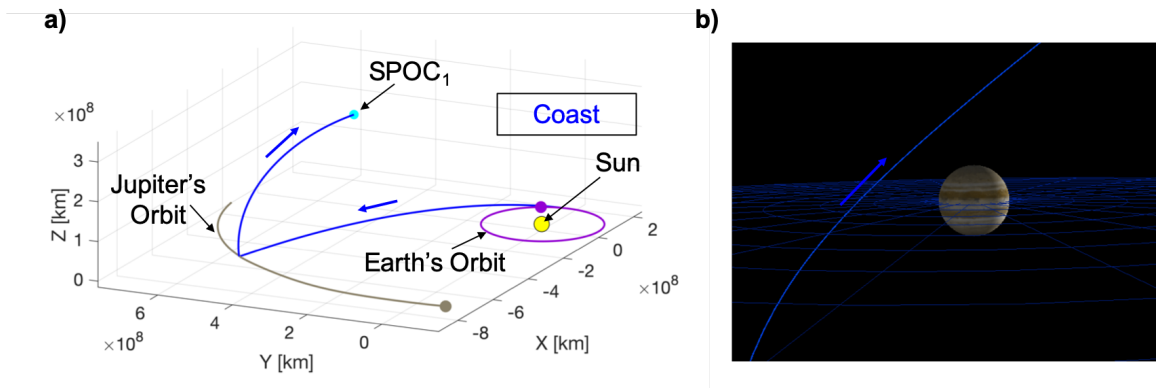


Figure 4. a) Heliocentric view of the selected trajectory from launch to post-JGA and b) a close-up view of the JGA obtained from GMAT. The Launch-to-JGA phase of the mission concept includes only ballistic motion after launch.

From the preferred set of candidate trajectories, the solution highlighted by a red circle in Figure 3 is selected, departing from Earth on 9/28/2025 with a $C_3 = 130.29 \frac{km^2}{s^2}$. Although this C_3 value would traditionally be considered large, it is feasible based on the predicted capabilities of the Falcon Heavy. The selected trajectory encounters Jupiter approximately 463 days later on 1/4/2027. After the Jupiter flyby, the spacecraft achieves a heliocentric inclination equal to 88.38° with respect to the ecliptic plane, an eccentricity equal to 0.714, and a radius of periapsis equal to 0.895 AU. A heliocentric view of the selected trajectory from launch to post-JGA for the spacecraft $SPOC_1$ is depicted in Figure 4a) in a Sun-centered inertial frame while a close-up view of the JGA is plotted via GMAT in Figure 4b). The selected trajectory achieves a nearly polar heliocentric orbit and provides an initial design point for developing the JGA-to-Operational-Orbit trajectory design of the mission concept.

DESIGN APPROACH: JUPITER GRAVITY ASSIST TO OPERATIONAL ORBIT

After the JGA, the SEP system is used to achieve a low-eccentricity heliocentric orbit via propulsive maneuvers. The trajectory solution selected from the Launch-to-JGA analysis achieves a heliocentric eccentricity equal to 0.714 with a periapsis radius equal to 0.895 AU and an apoapsis radius equal to 5.363 AU immediately after the JGA. However, the semi-major axis of the final operational orbit is required to be less than 1 AU and the final eccentricity is required to be less than or equal to 0.05. Therefore, the primary objective of the propulsive maneuvers is to reduce the eccentricity of the heliocentric orbit after the JGA and lower the apoapsis radius without adjusting the inclination. The most efficient maneuver location to reduce the apoapsis radius of the orbit is centered around periapsis with the thrust directed in the anti-velocity direction.¹⁶ Additionally, maneuvers that are executed far from the Sun are less effective than maneuvers executed closer to the Sun when using a SEP system; the thrust and mass flow rate are dependent on the available power, which is lower at farther distances from the Sun.¹⁵ Therefore, the initial guess for the propulsive maneuvers are placed around periapsis with thrust vectors primarily in the anti-velocity direction to rapidly reduce both the eccentricity and semi-major axis of the initial post-JGA orbit.

A low-complexity thrust profile to achieve a nearly circular heliocentric orbit is developed using an initial guess constructed via heuristics and a multiple shooting corrections scheme.¹⁸ A SEP-enabled two-body model with the Sun as the central body is used as the dynamical model. To avoid

numerical sensitivities during corrections, a nondimensionalization scheme is introduced. Distance quantities are normalized using the distance between the Sun and the Earth, the mass of the spacecraft is normalized using its initial wet mass, and time quantities are nondimensionalized such that the mean motion of the Sun-Earth system is unity. An initial guess for the trajectory is then developed using a series of nodes, coast arcs, and thrust arcs based on the true anomaly as depicted in Figure 5. The trajectory is discretized into a sequence of n arcs, each described by the state, time, and mass of its initial node along with the integration time of the arc and whether the thrusters are activated: for a SEP-enabled arc, the unit thrust vector components are required. The initial guess includes two maneuvers centered around periapsis that each contain five individual thrust arcs. Each thrust arc has a constant unit thrust vector direction defined in the VNC frame of the spacecraft relative to the Sun. The inner thrust arcs for each maneuver are initialized with thrust vectors entirely in the anti-velocity direction to reduce both the eccentricity and apoapsis of the orbit. The outer thrust arcs for each maneuver are primarily in the anti-velocity direction but also incorporate small thrust components in opposite conormal directions on either side of periapsis to further reduce the eccentricity of the orbit. Finally, the initial heliocentric state of the trajectory after the JGA is fixed, to correspond to the trajectory solution selected in the Launch-to-JGA analysis.

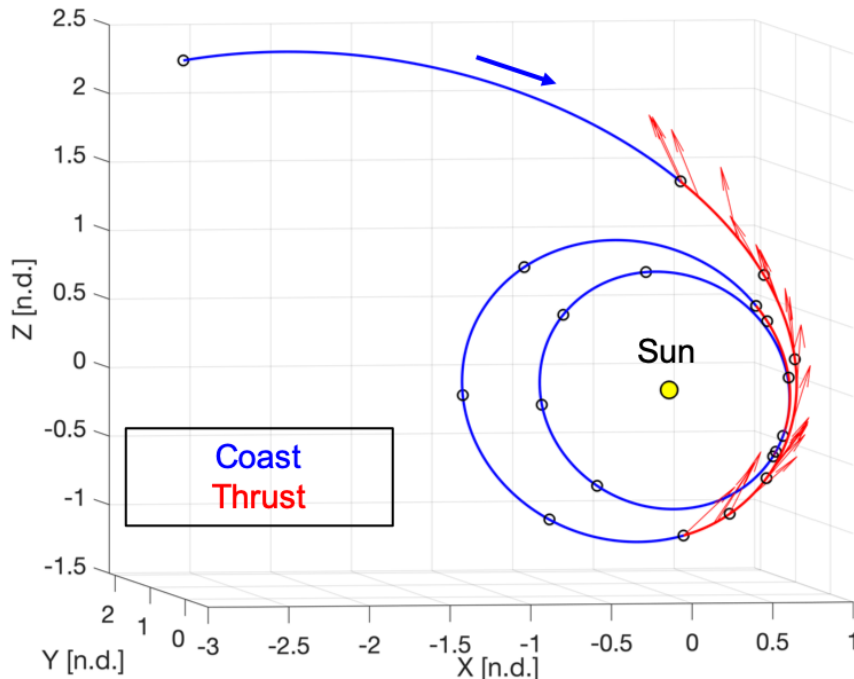


Figure 5. Initial guess for the SEP maneuvers used to achieve a nearly circular heliocentric orbit. The initial heliocentric state is obtained after the JGA from the trajectory solution selected in the Launch-to-JGA analysis, coast arcs are denoted in blue, and thrust arcs are denoted in red.

Given an initial guess and trajectory discretization, a free variable vector, \vec{X} , is defined such that \vec{X} contains all of the parameters defining the trajectory to be adjusted by the multiple shooting corrections algorithm. The full state and mass of the spacecraft at the initial node are fixed. However, the nondimensional integration time, $\Delta\tilde{t}$, of the first arc is allowed to vary. Thus, the component of

the free variable vector corresponding to the first arc is defined as:

$$\vec{X}_{InitialNode} = [\Delta\tilde{t}_1] \quad (8)$$

Then, if the i^{th} arc does not leverage a maneuver, the component of the free variable vector corresponding to the arc is defined as:

$$\vec{X}_i = [\tilde{q}_i, \tilde{m}_i, \tilde{P}_i, \Delta\tilde{t}_i] \quad (9)$$

where, at the initial node along the arc, \tilde{q}_i is the nondimensional state of the spacecraft relative to the Sun, \tilde{m}_i is the nondimensional mass of the spacecraft, and \tilde{P}_i is the nondimensional epoch. However if the thrusters are activated along the i^{th} arc, the component of the free variable vector corresponding to the arc is defined as:

$$\vec{X}_i = [\tilde{q}_i, \tilde{m}_i, \tilde{P}_i, \Delta\tilde{t}_i, \hat{u}_i] \quad (10)$$

The individual components of the free variable vectors, defined for each arc, are then combined to define the full free variable vector, \vec{X} , equal to:

$$\vec{X} = [\vec{X}_{InitialNode} \quad \cdots \quad \vec{X}_i \quad \cdots \quad \vec{X}_n]^T \quad (11)$$

The multiple shooting corrections algorithm iteratively updates this full free variable vector to find a solution that satisfies a set of constraints. A constraint vector, $\vec{F}(\vec{X})$, is defined such that the desired value of each constraint is zero. Full state, time, and mass continuity is constrained between each arc of the trajectory. Additionally, if the thrust is activated along an arc, the unit thrust vector is constrained to have a magnitude equal to unity. A final constraint is then included to restrict the heliocentric eccentricity of the final orbit to a specified value. These constraints are used in the multiple shooting corrections algorithm to ensure that, if a solution is found, the solution is continuous and achieves the desired operational orbit eccentricity within a numerical tolerance.

Using \vec{X} and $\vec{F}(\vec{X})$, a multiple shooting corrections algorithm finds a solution by iteratively updating \vec{X} until the magnitude of $\vec{F}(\vec{X})$ is less than a specified tolerance, such as 10^{-11} . In this application there are more free variables than constraints. Thus, at the k^{th} iteration, the free variable vector is updated using a minimum-norm solution as:

$$\vec{X}_{k+1} = \vec{X}_k - D\vec{F}(\vec{X}_k)^T [D\vec{F}(\vec{X}_k)D\vec{F}(\vec{X}_k)^T]^{-1} \vec{F}(\vec{X}_k) \quad (12)$$

where $D\vec{F}(\vec{X})$ is the derivative of $\vec{F}(\vec{X})$ with respect to \vec{X} . $D\vec{F}(\vec{X})$ is computed numerically via forward finite differencing. The final converged solution produced by the multiple shooting corrections algorithm is then used as the initial guess for the trajectory in a SEP-enabled point mass ephemeris model with the Sun as the central body: a process commonly known as continuation. The corrections algorithm is executed again using the initial guess in the higher fidelity dynamical model and the converged solution is then input to GMAT to produce a full end-to-end trajectory.

RESULTS: END-TO-END TRAJECTORY DESIGN

Leveraging the systematic design techniques outlined for each phase of the mission, a full end-to-end trajectory solution for a single spacecraft in the SPOC mission concept is input to GMAT using a SEP-enabled point mass ephemeris model including the Sun, Earth, Mars, Jupiter, and Saturn. The baseline trajectory solution for the first SPOC spacecraft departs Earth with a $C_3 = 130.29 \frac{km^2}{s^2}$, encounters Jupiter at a periapsis radius of approximately 6.3 Jupiter radii, and achieves a post-JGA heliocentric inclination equal to 88.38° with respect to the ecliptic plane. Table 2 lists the epoch of the Earth departure, JGA, and operational orbit arrival for the baseline trajectory solution as well as the time from launch to the operational orbit and the required propellant mass, satisfying the trajectory design requirements. The orbit parameters of the final operational orbit are listed in Table 3. Two SEP maneuvers centered around periapsis are leveraged to reduce the heliocentric eccentricity of the post-JGA orbit from 0.714 to approximately 0.04 as displayed in Figure 6. This figure provides a heliocentric view of the full trajectory for the first SPOC spacecraft displayed with respect to Venus, Earth, and Jupiter’s orbits in a Sun-centered inertial frame. Coast arcs are denoted in blue, thrust arcs are denoted in red, and the final operational orbit of the spacecraft is denoted in black. The spacecraft departs Earth, cruises towards Jupiter, completes a ballistic JGA, executes a maneuver centered around periapsis, coasts in an intermediate orbit, and finally executes a second maneuver centered around periapsis to reach the final operational orbit. The unit thrust vector direction of the spacecraft varies throughout each maneuver. However, it is primarily directed in the anti-velocity direction of the spacecraft’s VNC frame defined relative to the Sun to reduce the eccentricity and semi-major axis of the orbit. When away from periapsis, small components in the conormal direction up to approximately 27.2° off the anti-velocity direction are introduced to further reduce the eccentricity of the orbit. Additionally, Figure 7 shows the distance of the spacecraft from the Sun as a function of mission elapsed time, which is important to analyze because the efficiency of the SEP maneuvers depends on the distance of the spacecraft with respect to the Sun. The first maneuver starts at approximately 1.53 AU and ends at 1.07 AU from the Sun with a maneuver duration of 5.19 months. Then, the second maneuver starts at approximately 0.89 AU and ends at 0.84 AU from the Sun with a maneuver duration of 1.93 months. The final operational orbit is reached upon completion of the second maneuver, approximately 5.51 years after launch which is well below the maximum of 8 years specified in the design requirements.

Obtaining polar vantage points of the Sun to study its magnetic field is the primary objective of the SPOC mission concept. Derived from this objective, a maximum solar latitude greater than 75° is required for each spacecraft in the constellation during its operational orbit. Figure 8a) displays the distance of one SPOC spacecraft from the Sun as a function of its solar latitude while Figure 8b) depicts the solar latitude of the spacecraft as a function of mission elapsed time. The maximum

Table 2. Mission Timeline of the First SPOC Spacecraft

Event	Epoch
Launch from Earth	9/28/2025
Jupiter Gravity Assist	1/4/2027
Operational Orbit Arrival	4/1/2031
Time to Operational Orbit (yrs)	5.51
Required Propellant Mass (kg)	249.29

Table 3. Final Heliocentric Operational Orbit Parameters of the First SPOC Spacecraft

Parameter	Value
Semi-major Axis (a)	0.868 AU
Eccentricity (e)	0.0405
Inclination (i)	88.38°
Orbit Period	0.81 years

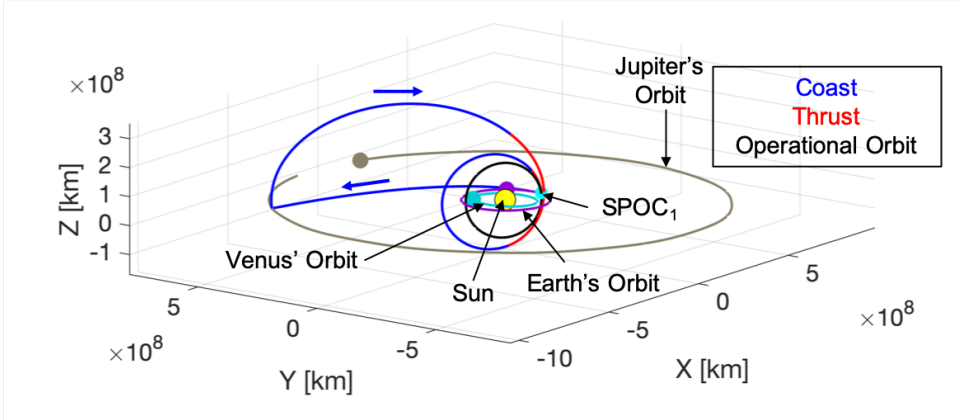


Figure 6. Heliocentric view of the full trajectory for the first SPOC spacecraft with respect to Venus, Earth, and Jupiter’s orbits.

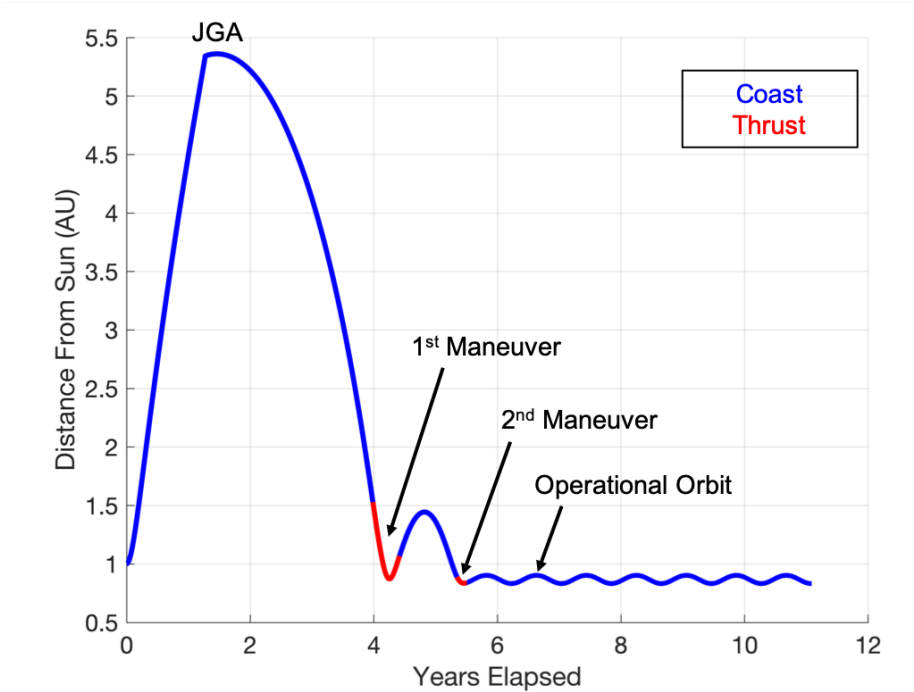


Figure 7. Distance of the first SPOC spacecraft from the Sun as a function of mission elapsed time.

solar latitude achieved in the operational orbit is $\pm 85.07^\circ$. Before reaching the operational orbit, the first maneuver is executed while the spacecraft is near the northern pole of the Sun and the maneuver ends just before the maximum latitude is reached in the southern hemisphere of the Sun; thrusting through this polar pass may limit the science capabilities of the spacecraft during the first two polar passes of the Sun. However, the second burn is not executed at high latitudes and therefore the science observations and operations will not be limited through the remaining polar passes of the mission. Figures 9a) and 9b) offer additional insight into the maneuvers by depicting the thrust and mass flow rate of the SEP system with respect to mission elapsed time respectively. The first maneuver begins while the spacecraft is farther than 1 AU from the Sun and therefore the three XIPS-25 thrusters do not have enough power to produce the maximum thrust of 495 mN for the entire duration of the maneuver. However, the entire second maneuver is executed while the spacecraft is less than 1 AU from the Sun and the SEP system achieves its maximum thrust. Figure 9b) plots the corresponding depletion of the propellant mass for each maneuver: a total of 249.29 kg of fuel is used for these maneuvers. Therefore, 39.71 kg of propellant remains once the spacecraft reaches its final operational orbit, resulting in a propellant mass margin equal to 15.93%. This analysis is focused on developing a single feasible solution to enable the SPOC mission concept. However, optimal solutions can be explored in future analyses to increase the propellant margin. Nevertheless, the baseline trajectory solution developed for the first SPOC spacecraft satisfies the requirements of the SPOC mission concept and is leveraged to develop constellation phasing strategies.

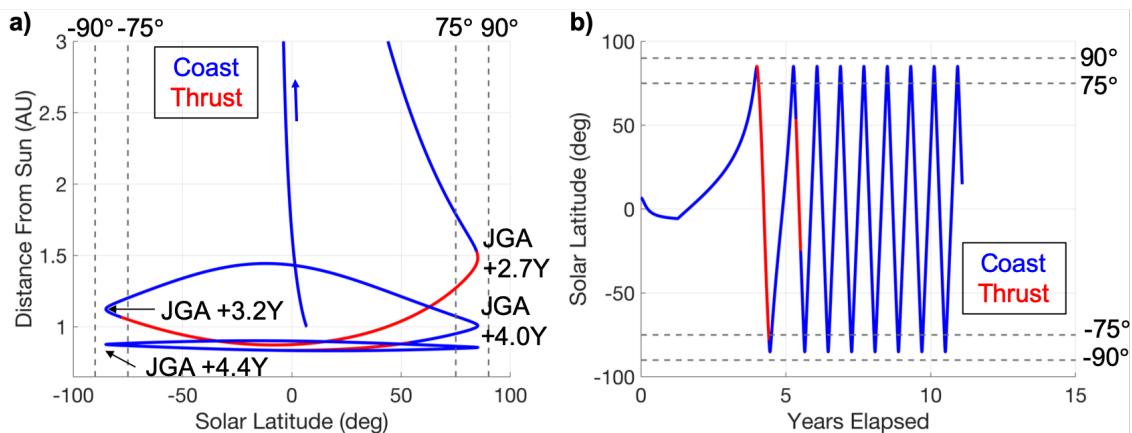


Figure 8. a) Distance of the first SPOC spacecraft from the Sun as a function of its solar latitude and b) the solar latitude of the spacecraft as a function of mission elapsed time.

RESULTS: CONSTELLATION PHASING

Straightforward strategies for phasing a constellation of solar observing spacecraft are designed using the baseline trajectory solution presented for a single spacecraft as a reference. The following two constellation phasing strategies are evaluated: (1) multiple spacecraft launched in a single launch opportunity and (2) multiple launches in separate launch opportunities. The first strategy assumes two SPOC spacecraft are launched within the same launch opportunity and, therefore, have nearly identical transfer trajectories from Earth to Jupiter and JGA geometries. To achieve a phase difference in the final operational orbit, the first spacecraft executes the nominal maneuvers of the baseline trajectory while the second spacecraft completes an extra revolution in an intermediate or-

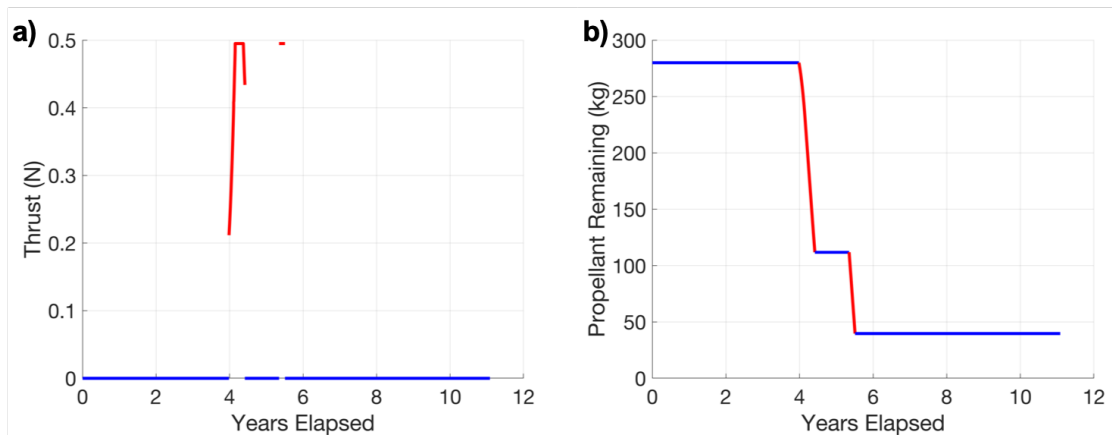


Figure 9. a) Thrust produced by the SEP system and b) propellant remaining for the first SPOC spacecraft as a function of mission elapsed time.

bit before executing the second burn. Conversely, the second strategy assumes two SPOC spacecraft are launched during separate launch opportunities separated by approximately 400 days, which corresponds to the synodic period of Earth and Jupiter. The delay between the launches results in a right ascension phasing between the final heliocentric orbits achieved by each spacecraft. Both phasing strategies offer viable solutions to develop an operational constellation of solar observatories.

Multiple Spacecraft in a Single Launch Opportunity

The baseline trajectory for a single SPOC spacecraft requires two propulsive maneuvers separated by an intermediate orbit before reaching the final operational orbit, enabling natural phasing of multiple spacecraft. First, two spacecraft are assumed to launch during the same launch opportunity and follow similar trajectories from Earth through the JGA. Following the JGA, the first spacecraft executes the nominal trajectory displayed in Figure 6 while the second spacecraft completes an extra revolution in the intermediate transfer orbit before completing the second maneuver. However, the resulting true anomaly phase difference in the final operational orbit between the two spacecraft depends on the ratio of the periods of the intermediate and operational orbits. In fact, the trajectory in Figure 6 is designed to achieve a 3:2 resonance between the period of the intermediate orbit and the period of the operational orbit. As a result, the spacecraft achieve a phase difference of approximately 180° in true anomaly when the second spacecraft delays its second maneuver by completing an additional revolution along the intermediate orbit. An example of this phasing strategy is displayed in Figure 10: in Figure 10a) the distance of each spacecraft from the Sun throughout the mission is plotted and portrays the additional revolution the second spacecraft spends in the intermediate orbit before executing the second maneuver. The coast arcs of the first spacecraft are denoted in blue, the coast arcs of the second spacecraft are denoted in black, and the thrust arcs for both spacecraft are denoted in red. Figure 10b) depicts the latitude of each spacecraft throughout their respective trajectories, achieving a phase difference of 176.00° in the final operational orbit. The time required for phasing the second spacecraft delays its arrival to the operational orbit by approximately 1.22 years. Consequently, the operational redundancy of the mission concept is also delayed by the time required for phasing. Thus, 6.73 years are required to achieve the constellation configuration. However, the time spent in the intermediate orbit could provide more opportunities for secondary science observations. This constellation phasing strategy offers

a straightforward solution to develop the constellation of SPOC spacecraft but relies on the proper sizing of the intermediate orbit to achieve a desirable phasing time and requires the second spacecraft to spend an additional 1.22 years in transit to its final destination. Constraining the period of the intermediate orbit relative to the operational orbit introduces an additional degree of complexity in developing SEP maneuvers to achieve an operational orbit and may require additional propellant mass; however, the mission requirements can still be satisfied.

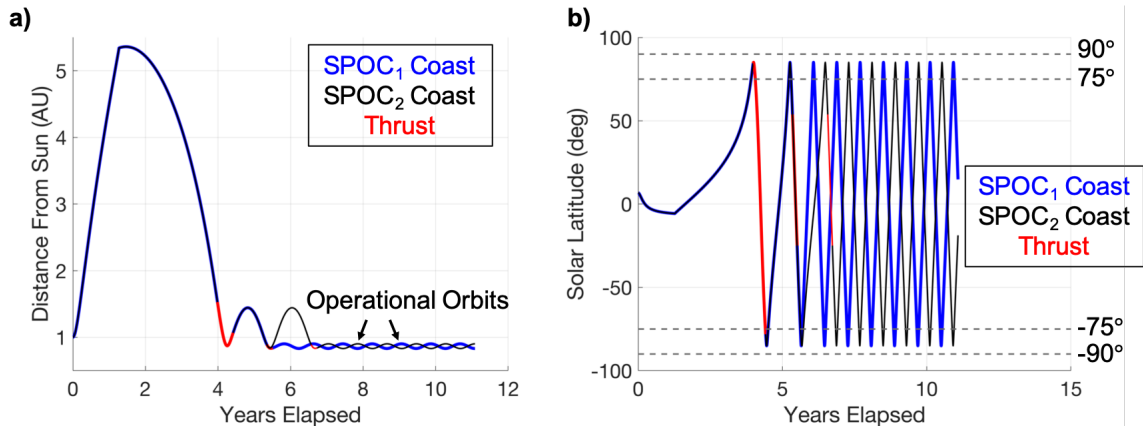


Figure 10. a) Distance of the first and second SPOC spacecraft from the Sun and b) the solar latitudes of each spacecraft as a function of mission elapsed time.

Multiple Launches in Separate Launch Opportunities

Leveraging the synodic period of Earth and Jupiter enables a constellation phasing strategy that results in both a right ascension and true anomaly phase difference between two spacecraft. Similar Earth to Jupiter transfer opportunities separated by approximately 400 days are revealed in Figure 1 due to a repetition of geometries consistent with the synodic period of Earth and Jupiter. A second transfer trajectory departing the Earth on 10/23/2026 with a $C_3 = 129.75 \frac{km^2}{s^2}$ encounters Jupiter on 2/16/2028. The same Jupiter B-plane targets and initial SEP maneuver design strategy used to compute the baseline trajectory are also used to compute this end-to-end trajectory. A heliocentric view of this trajectory for the second SPOC spacecraft as well as the baseline trajectory for the first SPOC spacecraft is depicted in Figure 11 relative to Venus, Earth, and Jupiter's orbits in a Sun-centered inertial frame. The final heliocentric orbit parameters for the second SPOC spacecraft are listed in Table 4 with the inclination measured with respect to the ecliptic plane. This second spacecraft reaches its operational orbit on 5/26/2032, which results in a phasing time of 1.15 years (i.e. 6.66 years to achieve the constellation configuration) and a phasing angle of 149.53° in terms of true anomaly. Similar to the first phasing strategy, the operational redundancy of the mission concept is delayed due to the phasing time required for the second spacecraft. This strategy requires further investigation to achieve a phasing in terms of true anomaly closer to 180° . Nevertheless, this phasing strategy also provides a 31.55° difference in the right ascension, Ω , between the two operational orbits as depicted in Figure 11. The phasing achieved via multiple launches in separate launch opportunities not only supplies differences in solar latitude between two spacecraft, but also provides different longitudinal views of the Sun.

Table 4. Final Heliocentric Operational Orbit Parameters of a Second SPOC Spacecraft

Parameter	Value
Semi-major Axis (a)	0.868 AU
Eccentricity (e)	0.0399
Inclination (i)	90.29°
Orbit Period	0.81 years

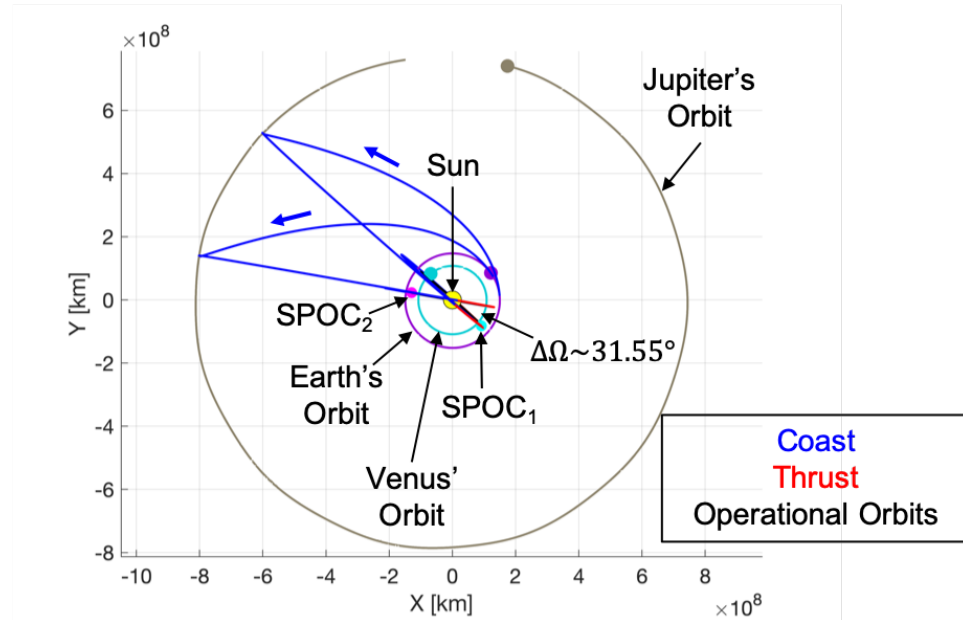


Figure 11. Heliocentric view of the full end-to-end trajectories for two SPOC spacecraft launched in different launch opportunities separated by the synodic period of Earth and Jupiter.

CONCLUSION

Regularly obtaining polar viewpoints of the Sun is essential for developing complete and accurate solar magnetic field models and solar wind forecasts. In pursuit of this goal, the University of Colorado Boulder’s SWx TREC and Ball Aerospace are developing the SPOC mission concept to construct a constellation of solar observatories via a JGA and SEP maneuvers that obtain regular and complete measurements of the Sun’s poles and off-Sun-Earth-line viewpoints. This paper presents a systematic trajectory design process used to develop the current baseline solution for a single spacecraft in the SPOC concept. The baseline trajectory achieves a heliocentric orbit with an inclination equal to 88.38° with respect to the ecliptic plane, an eccentricity equal to 0.0405, and a semi-major axis equal to 0.868 AU within 6 years after launch using a propellant mass of 249.29 kg for a spacecraft with a dry mass of 620 kg. This solution requires a launch vehicle capable of delivering a 900 kg spacecraft to Jupiter with a C_3 of $130.29 \frac{km^2}{s^2}$, such as the Falcon Heavy. Two candidate phasing strategies are also designed and discussed for a simplified representation of a constellation via two spacecraft. Achieving a constellation of two spacecraft is critical for both operational redundancy and obtaining simultaneous measurements of both the north and south pole of

the Sun. Launching two spacecraft in a single launch opportunity provides a straightforward and intuitive phasing approach via an intermediate transfer orbit designed with a resonance with respect to the final operational orbit. However, this approach adds additional complexity in the SEP maneuver design process to properly size the intermediate orbit while also achieving the desired operational orbit. Conversely, launching two spacecraft in separate launch opportunities provides both latitudinal and longitudinal phasing of the spacecraft around the Sun. This approach adds complexity in achieving a specific phasing angle in terms of true anomaly. Both constellation phasing strategies delay the operational redundancy of the mission concept by over a year due to the phasing time required for the second spacecraft. However, both approaches present feasible strategies that can be used to enable the SPOC mission concept and obtain both regular and complete measurements of the Sun to improve solar weather forecasting.

ACKNOWLEDGMENT

This work is part of a collaboration between CU Boulder’s SWx TREC and Ball Aerospace & Technologies Corporation. The contributions in this paper were completed at the University of Colorado Boulder with funding from the Dean’s Graduate Assistantship, the Graduate Assistantship in Areas of National Need (GAANN) Fellowship, and SWx TREC.

REFERENCES

- [1] P. H. Scherrer, R. S. Bogart, R. I. Bush, J. T. Hoeksema, A. G. Kosovichev, J. Schou, W. Rosenberg, L. Springer, T. D. Tarbell, A. Title, C. J. Wolfson, and I. Zayer, *The Solar Oscillations Investigation - Michelson Doppler Imager*, pp. 129 – 188. Springer Netherlands, 1995.
- [2] P. H. Scherrer, J. Schou, R. I. Bush, A. G. Kosovichev, R. S. Bogart, J. T. Hoeksema, Y. Liu, T. L. Duvall, J. Zhao, A. M. Title, C. J. Schrijver, T. D. Tarbell, and S. Tomczyk, “The Helioseismic and Magnetic Imager (HMI) Investigation for the Solar Dynamics Observatory (SDO),” *Solar Physics*, Vol. 275, Jan 2012, pp. 207 – 227.
- [3] T. E. Berger, N. Duncan, J. Van Cleve, M. Shannon, N. Bosanac, I. Elliott, T. R. Smith, C. Sullivan, L. Upton, D. Baker, J. Thayer, S. Cranmer, C. Pankratz, and N. Hurlburt, “The Solar Polar Observing Constellation (SPOC) Mission - Combining Operational Full-Sun Magnetic Field Measurements with Polar Exploration,” *American Geophysical Union Fall Meeting*, Washington, D.C., December 2018.
- [4] J. A. Simpson, “Experiments Out of the Solar System: An Introduction to the Execliptic Mission,” *NASA Goddard Space Flight Center Proceedings of the Symposium on the Study of the Sun and Interplanetary Medium in Three Dimensions*, Greenbelt, MD, March 1976.
- [5] S. E. Gibson, A. Vourlidas, D. M. Hassler, L. A. Rachmeler, M. J. Thompson, J. Newmark, M. Velli, A. Title, and S. W. McIntosh, “Solar Physics from Unconventional Viewpoints,” *Frontiers in Astronomy and Space Sciences*, Vol. 5, 2018.
- [6] P. C. Liewer, D. Alexander, J. Ayon, A. Kosovichev, R. A. Mewaldt, D. G. Socker, and A. Vourlidas, “Solar Polar Imager: Observing Solar Activity from a New Perspective,” *Progress in Astronautics and Aeronautics: NASA Space Science Vision Missions*, Vol. 224, 2008, pp. 1–40.
- [7] A. Vourlidas, P. C. Liewer, M. Velli, and D. Webb, “Solar Polar Diamond Explorer (SPDEx): Understanding the Origins of Solar Activity Using a New Perspective,” <https://ui.adsabs.harvard.edu/abs/2018arXiv180504172V>, 2018.
- [8] T. Appourchaux, P. C. Liewer, M. Watt, D. Alexander, V. Andretta, F. Auchère, *et al.*, “POLAR Investigation of the Sun - POLARIS,” *Experimental Astronomy*, Vol. 23, No. 3, 2009, pp. 1079–1117.
- [9] D. Müller, R. G. Marsden, O. C. StCyr, and H. R. Gilbert, “Solar Orbiter: Exploring the Sun-Heliosphere Connection,” *Solar Physics*, Vol. 285, 2012.
- [10] E. C. Roelof, G. B. Andrews, P. C. Liewer, and D. Moses, “Telemachus: A Mission for a Polar View of Solar Activity,” *Advances in Space Research*, Vol. 34, No. 2, 2004, pp. 467–471.
- [11] J. Newmark and D. Hassler, “Concept Development for a Solar Polar Mission: SOLAR Polar EXplorer (SOLPEX),” *Polar Perspectives Workshop: Advancing Our Understanding of the Sun*, 2018.
- [12] K. Wenzel, R. Marsden, D. Page, and E. Smith, “Ulysses: The First High-Latitude Heliospheric Mission,” *Advances in Space Research*, Vol. 9, No. 4, 1989, pp. 25–29.
- [13] C. Russell and C. Raymond, *The Dawn Mission to Minor Planets 4 Vesta and 1 Ceres*. Springer, 2011.

- [14] D. M. Goebel, J. E. Polk, I. Sandler, I. G. Mikellides, and J. R. Brophy, "Evaluation of 25-cm XIPS Thruster Life for Deep Space Mission Applications," *31st International Electric Propulsion Conference*, Ann Arbor, MI, September 2009.
- [15] "General Mission Analysis Tool (GMAT) User Guide R2017a," <http://gmat.sourceforge.net/doc/R2017a/help-a4.pdf>, 2017.
- [16] J. E. Prussing and B. A. Conway, *Orbital Mechanics*. Oxford University Press, 2 ed., 2013.
- [17] D. A. Vallado, *Fundamentals of Astrodynamics and Applications*. Microcosm Press, 4 ed., 2013.
- [18] N. Bosanac, *Leveraging Natural Dynamical Structures to Explore Multi-Body Systems*. PhD dissertation, Purdue University, West Lafayette, IN, 2016.
- [19] C. H. Acton, "Ancillary Data Services of NASA's Navigation and Ancillary Information Facility," *Planetary and Space Science*, Vol. 44, No. 1, 1996, pp. 65–70.
- [20] "Launch Sites," <https://spaceflight.nasa.gov/shuttle/reference/shutref/sts/launch.html>, 2002.
- [21] J. A. Atchison, M. T. Ozimek, C. J. Scott, and F. E. Siddique, "Robust High-Fidelity Gravity-Assist Trajectory Generation Using Forward/Backward Multiple Shooting," *25th AAS/AIAA Space Flight Mechanics Meeting*, Williamsburg, VA, January 2015.
- [22] "Solar System Dynamics: HORIZONS Web-Interface," <https://ssd.jpl.nasa.gov/horizons.cgi>, 2019.